Hierarchical sliding mode control for a class of SIMO under-actuated systems[*]

by

Dianwei Qian, Jianqiang Yi and Dongbin Zhao

Laboratory of Complex Systems and Intelligence Science,
Institute of Automation, Chinese Academy of Sciences
Beijing, 100190, P.R. China
e-mail: dianwei.qian@ia.ac.cn, jianqiang.yi@ia.ac.cn, dongbin.zhao@ia.ac.cn

Abstract: A hierarchical sliding mode control approach is proposed for a class of SIMO under-actuated systems. This class of under-actuated systems is made up of several subsystems. Based on this physical structure, the hierarchical structure of the sliding surfaces is designed as follows. At first, the sliding surface of every subsystem is defined. Then the sliding surface of one subsystem is defined as the first layer sliding surface. The first layer sliding surface is used to construct the second layer sliding surface with the sliding surface of another subsystem. This process continues till the sliding surfaces of the entire subsystems are included. According to the hierarchical structure, the total control law is deduced by the Lyapunov theorem. In theory, the asymptotic stability of the entire system of sliding surfaces is proven and the parameter boundaries of the subsystem sliding surfaces are given. Simulation results show the feasibility of this control method through two typical SIMO under-actuated systems.

Keywords: control approaches, control applications, sliding mode control, under-actuated systems.

1. Introduction

Under-actuated systems are characterized by the fact that they have fewer actuators than the degrees of freedom to be controlled. They arise in extensive applications such as robots, manipulators and industrial equipments. Their dynamics often contains feedforward nonlinearities, non-minimum phase zero dynamics, nonholonomic constraints, and couplings, which make their control designs difficult (Spong, 1998). Recently, there has been an increasing attention to the respective control problems in theory and in practice.

In this study, we focus on a class of SIMO under-actuated systems. This class is rather large, including series, parallel or rotary inverted pendulum(s) systems, Pendubot, TORA, and so on. Such systems are often used for investigation of various control methods and for education in various concepts. Numerous control methods have been presented for them, such as energy-based control (Fantoni et al., 2000, and Xin et al., 2004), passivity-based control (Alleyne, 1998), hybrid control (Zhang and Tarn, 2002, 2003), intelligent control (Yi et al., 2002, and Lai et al., 1999), and partial feedback linearization techniques (Spong, 1995). Other results concerning them can be found in Rubi et al. (2002), Ortega et al. (2002), Fang et al. (2003), and Jung et al. (2004). Most papers proposed a control law for a specified system. There is lack of general results. In fact, a normal state space expression can depict this class. Thus, it is possible to design a control law for this class rather than one control law for one specified system.

Sliding mode control (SMC) is a powerful and robust nonlinear control method (Bartoszewicz, 2000, and Gao et al., 1993). It provides a good candidate for the control design of this class. But designing a conventional single layer sliding surface is not appropriate, because parameters of the sliding surface cannot be calculated directly according to Hurwitz condition as in linear systems (Wang et al., 2004). As far as physical structure is concerned, the class considered can be divided into several subsystems. Based on this structure, some control methods have been presented. Mon and Lin (Mon et al., 2002, and Lin et al., 2005) proposed a hierarchical fuzzy sliding mode control scheme. In the scheme, the controller parameters were modified by fuzzy logic. But they did not consider the stability of the subsystem sliding surfaces. Lo (Lo et al., 1998) designed a decoupled fuzzy sliding mode control law. By an intermediate variable, the whole system was decoupled into two levels. But this method could not be applied to n-level control ($n > 2$). As in the method presented by Mon and Lin, Lo also did not give a strict proof about the stability of the subsystem sliding surfaces. Yi (Yi et al., 2005) developed a cascade sliding mode control strategy. This controller was globally stable in the sense that all signals involved were bounded. But some controller parameters often needed to be switched to guarantee system stability. This might make it difficult to select controller parameters. Wang (Wang et al., 2004) designed a hierarchical sliding mode control law. The entire sliding surfaces were asymptotically stable. But the control law could not be general for the under-actuated systems with more subsystems than two. By considering the stability of subsystems, the parameters of the subsystem sliding surfaces in the above four papers were selected as positive constants. But none of them gave the upper boundaries of these parameters.

In this paper, a hierarchical sliding mode controller is developed for this class of SIMO under-actuated systems. In this approach, such an under-actuated system is divided into several subsystems according to its physical structure. The sliding surface of every subsystem is defined. Then, the sliding surface of one

subsystem is chosen as the first layer sliding surface. It is used to constructs the second layer sliding surface with the sliding surface of another subsystem. This process continues till all the subsystem sliding surfaces are included. Using Lyapunov stability theorem, the total control law is derived. Theoretically, the asymptotic stability of the entire system of sliding surfaces is proven. Further, we prove that the parameters of the subsystem sliding surfaces should be convergent to an open interval. To the best of the authors' knowledge, the upper boundaries of the parameters of the subsystem sliding surfaces are given for the first time. The simulation results show the feasibility of this control strategy through upswing control of a Pendubot system and stabilization control of a series double inverted pendulum system.

2. Design of the hierarchical sliding mode control

Consider the state space expression of the class of SIMO under-actuated systems with n subsystems in the following normal form:

$$\begin{cases} \dot{x}_1 = x_2 \\ \dot{x}_2 = f_1 + b_1 u \\ \dot{x}_3 = x_4 \\ \dot{x}_4 = f_2 + b_2 u \\ \quad \vdots \\ \dot{x}_{2n-1} = x_{2n} \\ \dot{x}_{2n} = f_n + b_n u \end{cases} \tag{1}$$

Here, $X = [x_1, x_2, \ldots, x_{2n}]^T$ is the state variable vector; f_i and b_i $(i = 1, 2, \ldots, n)$ are the nonlinear functions of the state vector; and u is the single control input.

Equation (1) can express the class of systems with different n, f_i and b_i. If $n = 2$, (1) can represent Pendubot, single inverted pendulum system and so on; if $n = 3$, it can express a series or parallel double inverted pendulum system; if $n = 4$, it can be considered as triple inverted pendulum system; and so on. Based on physical structure, the class of under-actuated systems can be divided into several subsystems. For example, a triple inverted pendulum system can be divided into four subsystems: upper pendulum, middle pendulum, lower pendulum, and cart. Such a system in (1) is made up of n subsystems. The ith subsystem includes the state variables x_{2i-1} and x_{2i}. Its state space expression is represented by

$$\begin{cases} \dot{x}_{2i-1} = x_{2i} \\ \dot{x}_{2i} = f_i + b_i u \end{cases} . \tag{2}$$

Define its sliding surface as

$$s_i = c_i x_{2i-1} + x_{2i}. \tag{3}$$

Here, c_i is a positive constant.

Differentiate s_i with respect to time t in (3), then, there exists

$$\dot{s}_i = c_i \dot{x}_{2i-1} + \dot{x}_{2i} = c_i x_{2i} + f_i + b_i u. \tag{4}$$

Let $\dot{s}_i = 0$ in (4), the equivalent control of the ith subsystem is obtained as

$$u_{eqi} = -(c_i x_{2i} + f_i)/b_i. \tag{5}$$

According to (3) and (5), a variety of hierarchical sliding mode control laws can be designed according to diverse combinations of the subsystem sliding surfaces (Yi et al., 2005, and Wang et al., 2004). Other control methods can also be combined with the hierarchical sliding mode method (Lin and Mon, 2005; Lo et al., 1998). In this paper, the hierarchical structure of the sliding surfaces is designed according to the following description. The sliding surface of one subsystem is chosen as the first layer sliding surface S_1. Then S_1 is used to construct the second layer sliding surface S_2 with the sliding surface of another subsystem. This process continues till all the subsystem sliding surfaces are included. Without loss of generality, s_1 is defined as S_1. The hierarchical structure of the sliding surfaces is shown in Fig. 1.
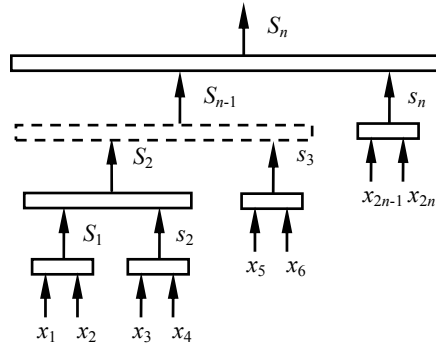

Figure 1. Hierarchical structure of the sliding surfaces

In Fig. 1, the ith layer sliding surface includes the entire information of the other $i-1$ layers sliding surfaces and the ith-subsystem sliding surface. As a result, the ith layer sliding surface is defined as follows:

$$S_i = \lambda_{i-1} S_{i-1} + s_i. \tag{6}$$

Here, λ_{i-1} $(i = 1, 2, \ldots, n)$ is constant and $\lambda_0 = S_0 = 0$.

Correspondingly, the ith layer sliding mode control law should include the information of the other $i-1$ lower layers sliding mode control laws and the

control law of the ith subsystem. Hence, the ith layer sliding mode control law is defined as

$$u_i = u_{i-1} + u_{eqi} + u_{swi}. \tag{7}$$

Here, $u_0 = 0$ and u_{swi} $(i = 1, 2, \ldots, n)$ is the switching control of the ith layer sliding surface.

The above control law (7) can be derived from the Lyapunov stability theorem. The Lyapunov function of the ith layer sliding surface is selected as

$$V_i(t) = S_i^2/2. \tag{8}$$

Differentiating V_i with respect to time t in (8), we obtain from (6):

$$\dot{V}_i = S_i \dot{S}_i = S_i(\lambda_{i-1}\dot{S}_{i-1} + \dot{s}_i). \tag{9}$$

Further, (10) can be deduced from (6):

$$S_i = \sum_{r=1}^{i} \Big(\prod_{j=r}^{i} a_j\Big) s_r. \tag{10}$$

Here, $a_j = \lambda_j$ $(j = 1, 2, \ldots, i - 1)$ is constant; and $a_i = 1$.
Hence, (11) is derived from (9) and (10):

$$\dot{V}_i = S_i \dot{S}_i = S_i \Big[\sum_{r=1}^{i} \Big(\prod_{j=r}^{i} a_j\Big) \dot{s}_r \Big]. \tag{11}$$

From (4), (5), (7), and (11), (12) is obtained:

$$\begin{aligned}
\dot{V}_i &= S_i\Big\{ \sum_{r=1}^{i} \Big[\Big(\prod_{j=r}^{i} a_j\Big) \cdot (c_r x_{2r} + f_r + b_r u_i) \Big] \Big\} \\
&= S_i\Big\{ \sum_{r=1}^{i} \Big[\Big(\prod_{j=r}^{i} a_j\Big) \cdot b_r \cdot \Big(\sum_{\substack{l=1 \\ l \neq r}}^{i} u_{eql} + \sum_{l=1}^{i} u_{swl} \Big) \Big] \Big\} \\
&= S_i \cdot \Big\{ \sum_{l=1}^{i} \Big[\sum_{\substack{r=1 \\ r \neq l}}^{i} \Big(\prod_{j=r}^{i} a_j\Big) b_r \Big] \cdot u_{eql} + \sum_{l=1}^{i} \Big[\sum_{r=1}^{i} \Big(\prod_{j=r}^{i} a_j\Big) b_r \Big] \cdot u_{swl} \Big\}. \tag{12}
\end{aligned}$$

By considering the stability of the ith layer sliding surface, let

$$\dot{S}_i = -k_i S_i - \eta_i \operatorname{sgn} S_i, \tag{13}$$

where k_i and η_i are positive constants.

From (12) and (13), the switching control law of the ith layer can be obtained as

$$u_{swi} = -\sum_{l=1}^{i-1} u_{swl} - \frac{\sum\limits_{l=1}^{i} \Big[\sum\limits_{\substack{r=1 \\ r \neq l}}^{i} \Big(\prod\limits_{j=r}^{i} a_j \Big) b_r \Big] u_{eql}}{\sum\limits_{r=1}^{i} \Big(\prod\limits_{j=r}^{i} a_j \Big) b_r} - \frac{k_i S_i + \eta_i \operatorname{sgn} S_i}{\sum\limits_{r=1}^{i} \Big(\prod\limits_{j=r}^{i} a_j \Big) b_r}. \tag{14}$$

Let $i = n$ in (7) and (14), then, there exists the hierarchical sliding mode control law as follows:

$$\begin{aligned} u_n &= \sum_{l=1}^{n-1} u_{swl} + u_{swn} + \sum_{l=1}^{n} u_{eql} \\ &= \frac{\sum\limits_{r=1}^{n} \Big(\prod\limits_{j=r}^{n} a_j \Big) b_r u_{eqr}}{\sum\limits_{r=1}^{n} \Big(\prod\limits_{j=r}^{n} a_j \Big) b_r} - \frac{k_n S_n + \eta_n \operatorname{sgn} S_n}{\sum\limits_{r=1}^{n} \Big(\prod\limits_{j=r}^{n} a_j \Big) b_r}. \end{aligned} \tag{15}$$

In (15), only the switching control of the last layer sliding mode controller works. The switching controls of the other n-1 lower layers are merged. In the reaching mode stage, when any state of a subsystem deviates from its own subsystem sliding surface, the switching control of the last layer will drive it back. Consequently, in the sliding mode stage, the system states keep sliding on the last layer sliding surface. Moreover, the states of every subsystem keep sliding on the subsystem sliding surface itself.

3. Stability analysis

Three theorems will be proven in this section. Theorem 1 is about the asymptotic stability of every layer sliding surface. Theorem 2 gives the stability analysis of the subsystem sliding surfaces. Further, we prove that the parameter of the ith-subsystem sliding surface should be convergent to an open interval in Theorem 3.

THEOREM 1 *Consider the class of under-actuated systems (1). If the control law adopted is (15) and the ith layer sliding surface is defined as (6), then S_i is asymptotically stable.*

Proof. Differentiate $V_i(t)$ with respect to time t in (8), then, from (13), we obtain

$$\begin{aligned} \dot{V}_i &= S_i \dot{S}_i \\ &= S_i(-k_i S_i - \eta_i \operatorname{sgn} S_i) \\ &= -k_i S_i^2 - \eta_i |S_i|. \end{aligned} \tag{16}$$

Integrating both sides of (16) yields

$$\int_0^t \dot{V}_i d\tau = \int_0^t (-k_i S_i^2 - \eta_i |S_i|) d\tau. \tag{17}$$

Further,

$$V_i(0) = V_i(t) + \int_0^t (k_i S_i^2 + \eta_i |S_i|) d\tau$$

$$\geqslant \int_0^t (k_i S_i^2 + \eta_i |S_i|) d\tau.$$

Hence

$$\lim_{t \to \infty} \int_0^t (k_i S_i^2 + \eta_i |S_i|) d\tau \leqslant V_i(0) < \infty. \tag{18}$$

According to Barbalat's lemma, there exists

$$\lim_{t \to \infty} (k_i S_i^2 + \eta_i |S_i|) = 0. \tag{19}$$

(19) means that $\lim_{t \to \infty} S_i = 0$. Namely, the ith layer sliding surface S_i is asymptotically stable. ∎

THEOREM 2 *Consider the class of under-actuated systems (1). If the control law adopted is (15) and the ith-subsystem sliding surface s_i is defined as (3), then s_i is asymptotically stable.*

Proof. From Theorem 1, we have

$$\lim_{t \to \infty} S_i = 0. \tag{20}$$

Let us prove that all the ith-subsystem sliding surfaces are asymptotically stable by contradiction. It is assumed that s_i is not asymptotically stable, namely

$$\lim_{t \to \infty} s_i \neq 0. \tag{21}$$

Calculating the limit of both sides of (10) yields

$$\lim_{t \to \infty} S_i = \lim_{t \to \infty} \sum_{r=1}^i \Big(\prod_{j=r}^i a_j \Big) s_r$$

$$= \sum_{r=1}^i \Big[\lim_{t \to \infty} \Big(\prod_{j=r}^i a_j \Big) s_r \Big]$$

$$= \sum_{r=1}^i \Big[\Big(\prod_{j=r}^i a_j \Big) \lim_{t \to \infty} s_r \Big] \neq 0. \tag{22}$$

(22) contradicts (20) that we have obtained from Theorem 1, so that the assumption (21) is false and the case opposite to (21) must be true. Therefore, the sliding surfaces of the entire set of subsystems are asymptotically stable. ∎

THEOREM 3 *For the class of under-actuated systems (1), adopting the control law (15), defining the ith-subsystem sliding surface (3) and assuming that all the state variables are equivalent infinitesimals of each other at a certain neighborhood of the origin, we have that the boundary of the parameter c_i should be $0 < c_i < |\lim_{X \to 0}(f_i/x_{2i})|$, where X is the state vector.*

Proof. When the states of the ith subsystem keep sliding on the subsystem sliding surface itself, the following equation can be obtained:

$$\begin{cases} s_i = c_i x_{2i-1} + x_{2i} = 0 & (a) \\ \dot{s}_i = c_i \dot{x}_{2i-1} + \dot{x}_{2i} = 0 & (b) \\ \dot{x}_{2i-1} = x_{2i} & (c) \\ \dot{x}_{2i} = f_i + b_i u_{eqi}. & (d) \end{cases} \tag{23}$$

1) Lower boundary of c_i

From (23a) and (23c), there exists

$$s_i = c_i x_{2i-1} + \dot{x}_{2i-1} = 0. \tag{24}$$

The eigenvalue of (24) should be negative for guaranteeing the stability of the ith-subsystem sliding surface. Thus, the lower boundary of c_i is $c_i > 0$.

2) Upper boundary of c_i

From (23b) and (23d), there exists

$$\dot{s}_i = c_i \dot{x}_{2i-1} + \dot{x}_{2i} = c_i x_{2i} + f_i + b_i u_{eqi} = 0. \tag{25}$$

Further, we have

$$c_i = |(f_i + b_i u_{eqi})/x_{2i}| \leqslant (|f_i| + |b_i u_{eqi}|)/|x_{2i}|. \tag{26}$$

When the states of the ith subsystem keep sliding on its own sliding surface and converge to a certain neighborhood of the origin, this subsystem can be treated as an autonomous system. Hence, we have the following inequality:

$$c_i \leqslant |f_i/x_{2i}|. \tag{27}$$

According to the limit concept of a multivariable function, $c_{i0} = |\lim_{X \to 0}(f_i/x_{2i})|$ can be calculated through the assumption that all the state variables are equivalent infinitesimals of each other at a certain neighborhood of the origin.

From part 1 and part 2, the boundary of the parameter c_i should be $0 < c_i < c_{i0}$. ∎

Theorem 3 is a necessary condition about the parameter c_i. If a self-adaptive control law is adopted, the value of c_i may not be in the open interval $(0, c_{i0})$ when the system states are far from the origin. But the parameter c_i will converge to this open interval as the system states converge to the origin. Although this theorem does not permit to calculate a precise value, it points out a direction for selecting the parameter c_i. Further, this theorem does not mean any number between 0 and c_{i0} could be selected as the value of the parameter c_i. The reason is that the different subsystem sliding surface parameters are coupled with each other in the controller. If one parameter is selected, other parameters, which still satisfy Theorem 3, have to be selected after trial and error by simulations. How to determine all the controller parameters directly may constitute another important research direction.

4.   Simulation results

Pendubot and series double inverted pendulum system are two typical under-actuated systems, which are often used to verify the feasibility of new control methods. Both of their dynamics have the similar expressions as (1) with different f_i, b_i, and n. In this section, the presented control method will be applied to upswing control of a Pendubot system and stabilization control of a series double inverted pendulum system. The demonstrations will show that this control method is feasible.

4.1.   Pendubot

The Pendubot system shown in Fig. 2 is made up of two subsystems: link 1 with an actuator (subscript 1) and link 2 without an actuator (subscript 2). The control objective of its upswing control is to swing up the Pendubot from the stable pending equilibrium point to its uppermost unstable equilibrium point and to stabilize at the uppermost unstable equilibrium point (Zhang and Tarn, 2002 and 2003; Wang et al., 2004).

The symbols in Fig. 2 are defined as follows: θ_1 is the angle of the link 1 with respect to the horizontal line; θ_2 is the angle of the link 2 with respect to the link 1; m_i, l_i and l_{ci} are the mass, length and distance to the centre of mass of link i, where $i = 1, 2$; τ_1 is the control torque. Let $n = 2$ in (1), then, the state space expression of the Pendubot system can be written as

$$\begin{cases} \dot{x}_1 = x_2 \\ \dot{x}_2 = f_1 + b_1 u \\ \dot{x}_3 = x_4 \\ \dot{x}_4 = f_2 + b_2 u. \end{cases} \tag{28}$$

Here, $x_1 = \theta_1 - \pi/2$) is the angle of the link 1 with respect to the vertical line; $x_3 = \theta_2$ is the angle of the link 2 with respect to the link 1; x_2 is the angular velocity of the link 1; x_4 is the angular velocity of the link 2; $u_{=}\tau_1$ is the single
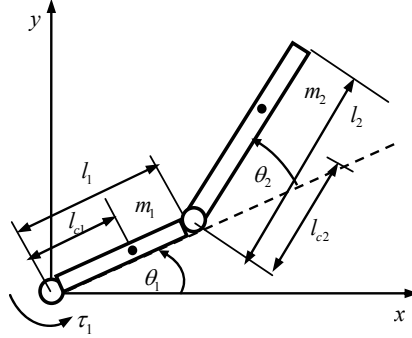
Figure 2. Structure of the Pendubot system

control input; the expressions for f_1, f_2, b_1 and b_2 are shown in Wang et al. (2004).

For comparisons, the parameters of the Pendubot are selected as q_1=0.0308kg · m^2, q_2=0.0106kg · m^2, q_3=0.0095kg · m^2, q_4=0.2086kg · m, q_5=0.0630kg · m, and the gravitational acceleration g=9.81m · s^{-2} which have appeared in Zhang and Tarn (2002 and 2003), Wang et al. (2004). According to Theorem 3, the boundaries of c_1 and c_2 are calculated as 66.97 and 68.68, whose expressions are given as

$$\begin{cases} c_{10} = g|(q_3q_5 - q_2q_4)/(q_1q_2 - q_3^2)| \\ c_{20} = g|[q_5(q_1 + q_3) - q_4(q_2 + q_3)]/(q_1q_2 - q_3^2|. \end{cases}$$

At last, the parameters of the hierarchical sliding mode controller are chosen as c_1=8.00, c_2=2.80, a_1=2.50, k_2=1.20, and η_2=0.10, after trial and error. The initial state vector X_0 is $[-\pi, 0, 0, 0]^T$ and the desired state vector X_d is $[0, 0, 0, 0]^T$.

Fig. 3 shows the angular curves. As Fig. 3 shows, this control strategy can realize the control objective in about 4 seconds. Fig. 4 displays the control torque. We can see from it that the largest control torque is about 4Nm.

Fig. 5 shows the entire sliding surfaces. As we have proven, not only every layer sliding surface is asymptotically stable, but also the sliding surfaces of the two subsystems possess the asymptotic stability.

By considering the property of equilibrium points, the control law in Wang et al. (2004) needed to be adjusted for different under-actuated systems. In practice, this may lead to a confusion. Further, Wang's method could only be applied for the under-actuated systems with two subsystems. Hence, the method here presented is more general. Compared with Wang's results, the angular curves and the control torque are smoother. During the future physical experiments, this advantage could decrease mechanical abrasions. The maximum of the control torque in Wang's results exceeded 4Nm, which was a little
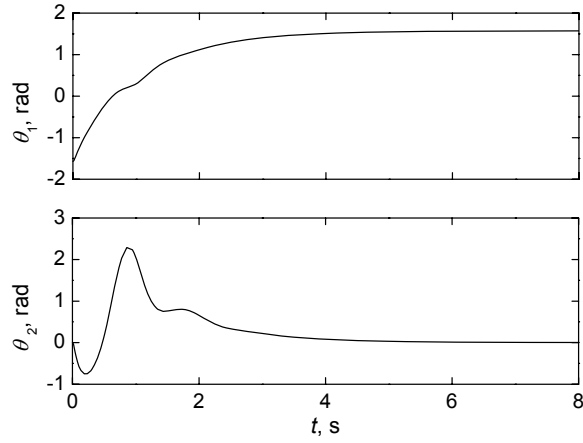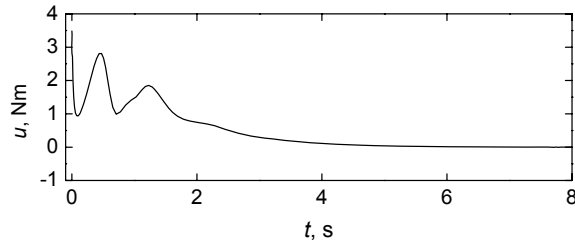
Figure 3. Angles of the Pendubot
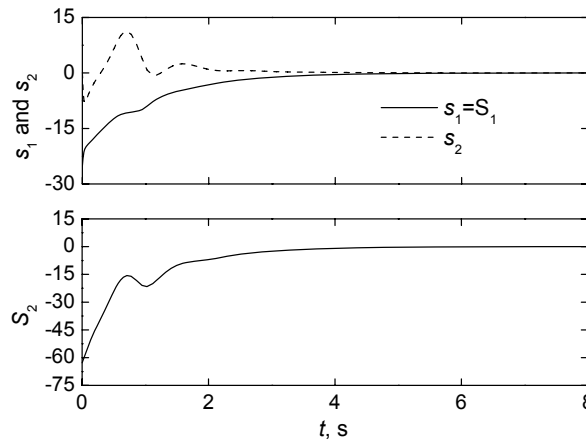

Figure 4. Control torque

Figure 5. Sliding surfaces

more than the performance shown in Fig. 4. But the presented control method
was not as robust as Wang's for upswing control of Pendubot system. Wang's
controller resisted a periodical disturbance of $y = 2\sin 10t$ and a step distur-
bance of 1 radian, which were out of reach for the present controller. In our
simulations, we found it could resist a periodical disturbance of $y = 0.4\sin 6\pi t$
and a step disturbance of 0.2 radian.

4.2. Series double inverted pendulum system

The series double inverted pendulum system is made up of double inverted
pendulums on a moving cart as is shown in Fig. 6. This system contains three
subsystems: the upper pendulum, the lower pendulum, and the cart. The
control objective of its stabilization control is to balance both of the pendulums
upright and to put the cart to the rail origin by moving the cart (Lin and Mon,
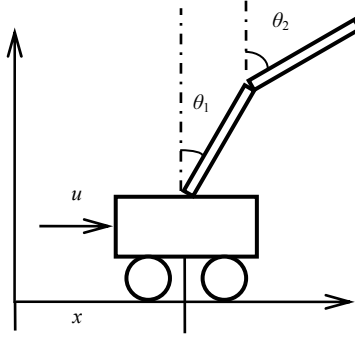2005).

Figure 6. Structure of the series double inverted pendulum system

The symbols in Fig. 6 are defined as follows: θ_1 is the lower pendulum angle
with respect to the vertical line; θ_2 is the upper pendulum angle with respect
to the vertical line; x is the cart position with respect to the origin; u is the
control force. Let $n = 3$ in (1), the state space expression of the series double
inverted pendulum system is described below:

$$\begin{cases} \dot{x}_1 = x_2 \\ \dot{x}_2 = f_1 + b_1 u \\ \dot{x}_3 = x_4 \\ \dot{x}_4 = f_2 + b_2 u \\ \dot{x}_5 = x_6 \\ \dot{x}_6 = f_3 + b_3 u. \end{cases} \tag{29}$$

Here, $x_1 = \theta_1$; $x_3 = \theta_2$; $x_5 = x$; x_2 is the angular velocity of the lower pendulum;

x_4 is the angular velocity of the upper pendulum; x_6 is the velocity of the cart; u is the single control input; f_i and b_i ($i = 1, 2, 3$) are given in Lo et al. (1998).

For simulative comparisons, the structural parameters of the series double inverted pendulum system are chosen as the cart mass M=1kg, the lower pendulum mass m_1=1kg, the upper pendulum mass m_2=1kg, the lower pendulum length l_1=0.1m, the upper pendulum length l_2=0.1m, the gravitational acceleration g=9.81m $\cdot$ s^{-2}, which have appeared in Lin and Mon (2005). According to Theorem 3, the boundaries of c_1, c_2 and c_3 are calculated as 294.39, 98.31 and 11.44, whose expressions are given as

$$
\begin{cases}
c_{10} = g\left| \dfrac{A^2(B/3 - m_2 l_2/4)}{(m_2/4 - A/3)(B^2 - AC) - m_2(B - Al_1)^2/4} \right| \\[3mm]
c_{20} = g\left| \dfrac{A^2(C - Bl_1)/2}{l_2[(m_2/4 - A/3)(B^2 - AC) - m_2(B - Al_1)^2/4]} \right| \\[3mm]
c_{30} = g\left| \dfrac{AB(B/3 - m_2 l_1/4) + A(Cm_2 - Bm_2 l_1)/2}{(m_2/4 - A/3)(B^2 - AC) - m_2(B - Al_1)^2/4} \right|
\end{cases}
$$

Here, $A = M + m_1 + m_2$, $B = m_1 l_1/2 + m_2 l_1$ and $C = m_1 l_1 l_1/3 + m_2 l_2 l_2$. The controller parameters are chosen as c_1=184.26, c_2=15.96, c_3=0.72, a_1= -0.06, a_2=0.45, k_3=1.50, and η_3=0.02, after trial and error. The initial state vector X_0 and the desired state vector X_d are $[\pi/6, 0, \pi/18, 0, 0, 0]^T$ and $[0, 0, 0, 0, 0, 0]^T$, which are the same as Lin and Mon (2005), Lo et al. (1998).

Fig. 7 shows the angular curves and the positional curve. The maximum distance of the cart with respect to the origin is about 0.6 m. Fig. 8 displays the control force applied to the cart.

Fig. 9 shows the curves of the subsystem sliding surfaces. We can see from it that the subsystem sliding surfaces are asymptotically stable as has been proven in Theorem 2. Fig. 10 displays the curves of the three layer sliding surfaces. It shows that every layer sliding surface can converge to zero as has been proven in Theorem 1.

Lo's control method could only realize two-level control. Consequently, that controller could only balance the double pendulums, but it failed to put the cart to the origin at the same time. Compared with Lo's results, our control objective is more difficult. In Lin's method, the controller parameters were modified by fuzzy logic. But the fuzzy rules were difficult to define. Moreover, the use of fuzzy logic made it difficult to analyze system stability. Compared with Lin's performance, the curves are smoother and the cart moves along a shorter distance in Fig. 7, although a bigger control force in Fig. 8 is needed in the beginning of the simulation, exceeding 200N. For most physical systems, it is very difficult to offer such a force or it is too expensive to offer it. On the other hand, such a force may make the input saturated, which may influence the reliable operation and acceptable performance of the control system. This weak point will restrict the control method in practice. Thus, solving of this issue is the problem to be addressed in future investigations.
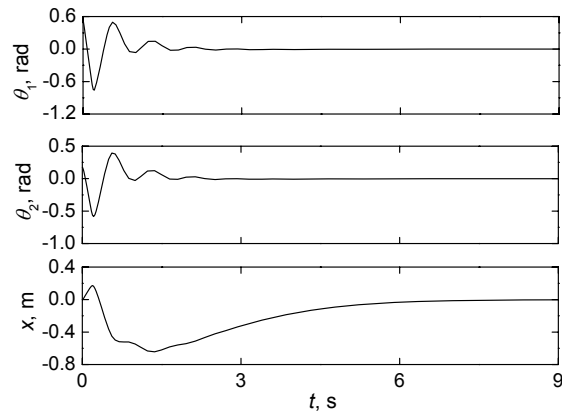
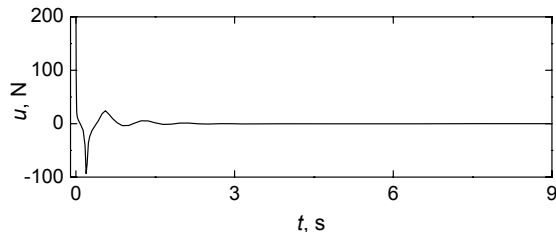Figure 7. Pendulum angles and cart position
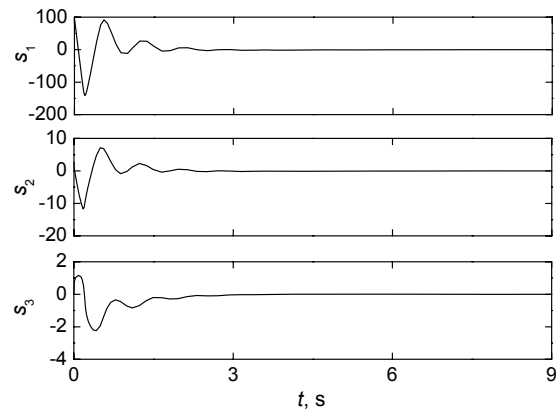
Figure 8. Control force

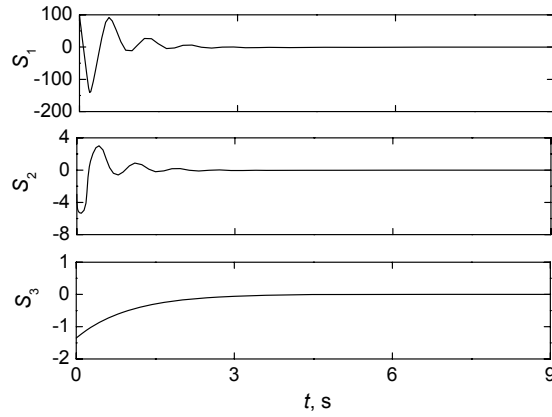Figure 9. Sliding surfaces of the three subsystems

Figure 10. Three layer sliding surfaces

Fig. 11 shows the stabilization domain of the initial angles of the two pendulums, for which the proposed hierarchical sliding mode controller can stabilize the pendulum system. Here, the horizontal axis and the vertical axis stand separately for the initial angles of the lower pendulum and the upper pendulum in degree. The initial angle of the lower pendulum is selected every $5°$ from $-40°$ to $40°$. For such a selected angle of the lower pendulum, the maximum angle of the upper pendulum that can be stabilized is plotted by the black filled triangle (▲) in Fig. 11. The initial values of the other state variables x_2, x_4, x_5, x_6 are all fixed to zeros. During the simulations, the complete stabilization time is within 6.0s and the cart position is in the interval [-1m, 1m].
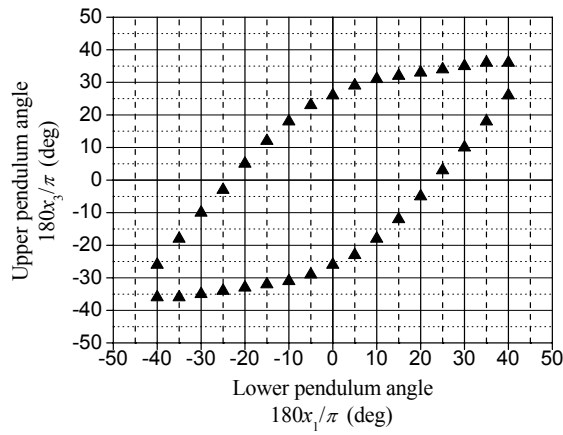

Figure 11. Stabilization domain

5.   Conclusions

The hierarchical sliding mode control scheme has been developed for a class of SIMO under-actuated systems. According to the physical structure of the class, the hierarchical sliding surfaces are designed. Using Lyapunov theorem, the total control law is derived. The asymptotic stability of the entire system of sliding surfaces is proven theoretically. To the best of the authors' knowledge, the upper boundaries on the parameter of the subsystem sliding surfaces are given for the first time. In the simulation examples, performance of this control method is demonstrated through upswing control of a Pendubot system and stabilization control of a series double inverted pendulum system. The two systems belong to the class considered, with different numbers of subsystems. The simulation results show the controller validity and generalization. This method can also be used to other under-actuated systems in the class besides the two demonstrated systems, like an overhead crane system, an Acrobot and so on. But there still exist some weak points in the presented control method, such as how to select the controller parameters, how to deal with the problem of the input saturation, and so on. The extensions and the physical experiment (Liu et al., 2005) are still the future issues.

Acknowledgement

References

ALLEYNE, A. (1998) Physical insights on passivity-based TORA control designs. *IEEE Transactions on Control Systems Technology* **6**, 436–439.

BARTOSZEWICZ, A. (2000) Chattering attenuation in sliding mode control systems. *Control and Cybernetics* **29**, 585-594.

FANG, Y., DIXON, W.E., DAWSON, D.M. and ZERGEROGLU, E. (2003) Nonlinear coupling control laws for an underactuated overhead crane system. *IEEE/ASME Transactions on Mechatronics* **8**, 418–423.

FANTONI, I., LOZANO, R. and SPONG, M.W. (2000) Energy based control of the pendubot. *IEEE Transactions on Automatic Control* **45**, 725–729.

GAO, W. and HUNG, J.C. (1993) Variable structure control of nonlinear systems: a new approach. *IEEE Transactions on Industrial Electronics* **40**, 45–55.

JUNG, S. and WEN, J.T. (2004) Nonlinear model predictive control for the swing-up of a rotary inverted pendulum. *ASME Journal of Dynamic Systems, Measurement and Control* **120**, 666–673.

LAI, X., SHE, J.H., OHYAMA, Y. and CAI, Z. (1999) Fuzzy control strategy for acrobots combining model-free and model-based control. *IEE Proceedings - Control Theory and Applications* **146**, 505–510.

LIN, C.M. and MON, Y.J. (2005) Decoupling control by hierarchical fuzzy sSliding mode controller. *IEEE Transactions on Control Systems Technology* **13**, 593–598.

LIU, D., YI, J., ZHAO, D. and WANG, W. (2005) Adaptive sliding mode fuzzy control for a two-dimensional overhead crane. *Mechatronics* **15** 505–522.

LO, J.C. and KUO, Y.H. (1998) Decoupled fuzzy sliding-mode control. *IEEE Transactions on Fuzzy Systems* **6**, 426–435.

MON, Y.J. and LIN C.M. (2002) Hierarchical fuzzy sliding-mode control. *Proceedings of 2002 IEEE International Conference on Fuzzy Systems* **1**, 656–661.

ORTEGA, R., SPONG, M.W., GOMEZESTERN, F. and BLANHENSTEIN, G. (2002) Stabilization of a class of underactuated mechanical systems via interconnection and damping assignment. *IEEE Transactions on Automatic Control* **47**, 1218–1233.

RUBI, J., RUBIO, A. and AVELLO, A. (2002) Swing-up control problem for a self-erecting double inverted pendulum. *IEE Proceedings - Control Theory and Applications* **149**, 169–175.

SPONG, M.W. (1998) Underactuated Mechanical Systems. *Lecture Notes in Control and Information Sciences* **230**, 135–150.

SPONG, M.W. (1995) The swing up control problem for the acrobot. *IEEE Control Systems Magazine* **15**, 49–55.

WANG, W., YI, J., ZHAO, D. and LIU, D. (2004) Design of a stable sliding-mode controller for a class of second-order underactuated systems. *IEE Proceedings - Control Theory and Applications* **151**, 683–690.

XIN, X. and KANEDA, M. (2004) New Analytical Results of the Energy Based Swinging up Control of the Acrobot. *Proceedings of the 43rd IEEE Conference on Decision and Control*, **1**, 704–709.

YI, J., YUBAZAKI, N. and HIROTA, K. (2002) A new fuzzy controller for stabilization of parallelt-type double inverted pendulum system. *Fuzzy Sets and Systems* **126**, 105–119.

YI, J., WANG, W., ZHAO, D. and LIU, X. (2005) Cascade sliding-mode controller for large-scale underactuated systems. *Proceedings of 2005 IEEE-RSJ International Conference on Intelligent Robots and Systems*, 301–306.

ZHANG, M. and TARN, T.J. (2002) Hybrid control of the pendubot. *IEEE-ASME Transactions on Mechatronics* **7**, 79–86.

ZHANG, M. and TARN, T.J. (2003) Hybrid switching control strategy for nonlinear and underactuated mechanical systems. *IEEE Transactions on Automatic Control* **48**, 1777–1782.